fermentation

MDPI

Article

Assessment of Growth Inhibition of Eugenol-Loaded Nano-Emulsions against Beneficial *Bifidobacterium* sp. along with Resistant *Escherichia coli* Using Flow Cytometry

Usman Majeed [1], Afshan Shafi [2,*], Muhammad Shahbaz [3], Kashif ur Rehman Khan [4], Khalid Javed Iqbal [5], Kashif Akram [6], Irfan Baboo [7], Shaukat Hussain Munawar [8], Muhammad Mazhar Munir [8], Rizwana Sultan [9], Hamid Majeed [6], Ilaria Cacciotti [10], Tuba Esatbeyoglu [11,*] and Sameh A. Korma [12,13]

1 College of Food Science and Technology, Northwest University, Xi'an 710069, China
2 Department of Food Science and Technology, Mian Nawaz Sharif Agriculture University, Multan 60000, Pakistan
3 Department of Zoology, Women University of Azad Jammu and Kashmir, Bagh 12500, Pakistan
4 Department of Pharmaceutical Chemistry, Faculty of Pharmacy, The Islamia University of Bahawalpur, Bahawalpur 63100, Pakistan
5 Department of Zoology, The Islamia University of Bahawalpur, Bahawalpur 63100, Pakistan
6 Department of Food Science and Technology, Cholistan University of Veterinary and Animal Sciences, Bahawalpur 63100, Pakistan
7 Department of Zoology, Cholistan University of Veterinary and Animal Sciences, Bahawalpur 63100, Pakistan
8 Department of Pharmacology and Toxicology, Cholistan University of Veterinary and Animal Sciences, Bahawalpur 63100, Pakistan
9 Department of Pathology, Cholistan University of Veterinary and Animal Sciences, Bahawalpur 63100, Pakistan
10 Department of Engineering, INSTM RU, University of Rome "Niccolò Cusano", Via Don Carlo Gnocchi 3, 00166 Roma, Italy
11 Department of Food Development and Food Quality, Institute of Food Science and Human Nutrition, Gottfried Wilhelm Leibniz University Hannover, Am Kleinen Felde 30, 30167 Hannover, Germany
12 Department of Food Science, Faculty of Agriculture, Zagazig University, Zagazig 44519, Egypt
13 School of Food Science and Engineering, South China University of Technology, Guangzhou 510641, China
* Correspondence: afshan.shafi@mnsuam.edu.pk (A.S.); esatbeyoglu@lw.uni-hannover.de (T.E.); Tel.: +92-3366708638 (A.S.); +49-5117625589 (T.E.)

Abstract: The intestinal tract microbiota influences many aspects of the dietary components on colon health and during enteric infections, thus, playing a pivotal role in the colon health. Therefore, the eugenol (EU) nano-emulsion effective concentration reported in our previous study against cancer cells should be explored for safety against beneficial microbes. We evaluated the sensitivity of *Bifidobacterium breve* and *B. adolescentis* against EU-loaded nano-emulsions at 0, 300, 600 and 900 µm, which were effective against colon and liver cancer cells. Both *B. breve* and *B. adolescentis* showed comparable growth ranges to the control group at 300 and 600 µm, as evident from the plate count experimental results. However, at 900 µm, a slight growth variation was revealed with respect to the control group. The real-time inhibition determination through flow cytometry showed *B. breve* viable, sublethal cells (99.49 and 0.51%) and *B. adolescentis* (95.59 and 0.15%) at 900 µm, suggesting slight inhibition even at the highest tested concentration. Flow cytometry proved to be a suitable quantitative approach that has revealed separate live, dead, and susceptible cells upon treatment with EU nano-emulsion against *Escherichia coli*. Similarly, in the case of *B. breve* and *B. adolescentis*, the cells showed only live cells that qualitatively suggest EU nano-emulsion safety. To judge the viability of these sublethal populations of *B. breve* and *B. adolescentis*, Fourier transforms infrared spectroscopy was carried out, revealing no peak shift for proteins, lipids, DNA and carbohydrates at 900 µm EU nano-emulsion compared to the control. On the other hand, EU-loaded nano-emulsions (900 µm)-treated *E. coli* showed a clear peak shift for a membrane protein, lipids, DNA and carbohydrates. This study provides insights to utilize plant phenols as safe medicines as well as dietary supplements.

check for updates

Citation: Majeed, U.; Shafi, A.; Shahbaz, M.; Khan, K.u.R.; Iqbal, K.J.; Akram, K.; Baboo, I.; Munawar, S.H.; Munir, M.M.; Sultan, R.; et al. Assessment of Growth Inhibition of Eugenol-Loaded Nano-Emulsions against Beneficial *Bifidobacterium* sp. along with Resistant *Escherichia coli* Using Flow Cytometry. *Fermentation* **2023**, *9*, 140. https://doi.org/10.3390/fermentation9020140

Academic Editors: Farhad Garavand and Eoin Byrne

Received: 22 December 2022
Revised: 25 January 2023
Accepted: 30 January 2023
Published: 31 January 2023

Keywords: *Bifidobacterium adolescentis*; dietary supplements; encapsulation; nano-emulsion; eugenol; bioavailability; flow cytometry; infrared spectroscopy

1. Introduction

Phytochemicals efficacy and bioavailability can be reduced due to poor aqueous solubility that leads to side effects [1]. Thus, the enhancement of the lipophilic compounds' solubility and bioavailability is still regarded as one of the most important challenges to be addressed in the drug development process [2,3]. Several efforts have been dedicated to the development of innovative herbal drugs delivery systems, taking into account the high costs associated with the synthetic drug-based approaches, as well as the correlated side effects and the decreased pathogen sensitivity due to multiple employments. Moreover, direct use of essential oils in the food system is not so popular, possibly due to its insolubility in water, potent odour, high volatility, susceptibility to oxidation and negative effects on the organoleptic properties of food [3]. Nanoencapsulation of essential oils in an effective polymeric matrix can conceal off-odour, reduce volatility, increase solubility and stability in water, and reduce contact with food matrices, improving bioavailability and bioactivity while providing effective release control [4]. It has been proposed that the most effective way to circumvent the aforementioned limitations is to nanoencapsulate essential oils into stable polymeric matrices [5]. Their end use in the food chain is possible due to the controlled release and protection against oxidation and evaporation that nanoencapsulation can provide [3]. Due to its unique properties such as abundance, biodegradability, cost-effectiveness, non-toxicity, and exceptional antibacterial and antioxidant activities, together with other polymers it has attracted much attention [4,5].

For example, yang et al. used encapsulated thyme essential oil against *Escherichia. coli* at two times lower concentration compared to unencapsulated [6]. In addition to this, some limitations, such as highly acidic pH during the oral consumption, cause the instability of the herbal bioactive and liver metabolism, leading to less or no effect, due to the drug levels below the therapeutic concentration in the blood [7,8]. Mansouri et al. fortified encapsulated thyme in mayonnaise as an antibacterial agent that was higher in quantity even after 30 days of storage [3]. To overcome the reported limits, the plant bioactive encapsulation has been proposed as a promising strategy to minimize their presystemic metabolism and side effects as a consequence of their accumulation to non-targeted areas.

Delivery systems such as nano-emulsions, micro-emulsions, liposomes, solid lipid nanoparticles and microspheres have been used to improve the hydrophobic nutraceuticals therapeutic efficacy by increasing their bioavailability and tissue specificity [3,6–8]. Among these, nano-emulsions loaded with oils from medicinal plants have shown enormous potential in terms of improved solubility, increased bioavailability and controlled release that prolong the biological activities in comparison to conventional emulsions and raw oils [9,10]. Due to their unique properties, including small size and high surface area, optical transparency, and delayed gravity separation and flocculation rate, nano-emulsions are excellent delivery methods for commercial applications. Emulsions [11], microencapsulation [7] and liposomes [6] are examples of lipid encapsulation systems in which lipids are entrapped by small- and large-molecule surfactants. A β-carotene nano-emulsion was developed by Mao et al. using both small (tween 20 and decaglycerol monolaurate) and large (octenyl succinate-starch and whey protein isolate) molecular surfactants [12]. They concluded that nano-emulsions formulated with octenyl succinate-starch and whey protein isolate were higher than tween 20 and decaglycerol monolaurate, but were more stable over time [12]. Purity gum 2000, a modified starch, was used to synthesize peppermint oil nano-emulsion, and Liang et al. found that it has high antibacterial activity against *L. monocytogenes* and *S. aureus* [13]. The ability of the emulsifier to dissolve the essential oil components in the aqueous phase determines the bactericidal activity of the essential oil components in the oil-water emulsion system [9]. Soy lecithin, pea protein,

sugar ester, and a mixture of glycerol monooleate and tween 20 were used to produce antimicrobial nano-emulsions of carvacrol, cinnamaldehyde and D-limonene [14]. They combined glycerol monooleate with emulsified tween 20 nano-emulsions and found that sugar esters improved the availability of antibacterial chemicals in water [14]. On the other hand, Terjung et al. found inconsistent results: they used tween 80 to create eugenol (EU)-loaded nano-emulsion and found that the aqueous phase contained fewer antimicrobial compounds, resulting in reduced bactericidal activity [15]. Therefore, nano-emulsions find their way into many industries such as pharmaceutics, food, cosmetics and other sectors. On the other hand, the use of nanocarriers led to detrimental effects on living cells as evident from performed in vitro studies [16]. In addition to nanocarriers, essential oils themselves can exert toxic effects on living cells if their effective concentrations are higher than the safe dose limits. Particularly, Thapa et al. reported toxic or growth-inhibitory effects of clove oil, EU and thymol against beneficial bacteria (*Faecalibacterium prausnitzii*) using the in vitro disc method, even if at high concentrations [5]. In detail, the investigated essential oils and their compounds showed inhibitory action against pathogenic bacteria at 300 ppm, whereas beneficial bacteria remained unaffected at this concentration. However, at the highest concentration (1000 ppm), beneficial bacteria (*F. prausnitzii*) showed a slight reduction in growth, even if quite insignificant compared to pathogenic bacterial growth inhibition. Similarly, another research group reported moderate inhibition of beneficial intestinal microbiota (*B. longum*, *B. breve*, *B. animalis* spp. *lactis*) at the highest concentration of essential oils (500 mg/L) [4]. Interestingly, for piglets weaned with microencapsulated thymol and cinnamaldehyde improved growth performance and gut microflora were revealed [17]. The objective of this study was to determine the safety of *Bifidobacterium* cells against EU nano-emulsions safety (IC_{50} < 500 μm) against colon and liver cancer cell lines as reported in our previous study [18].

2. Materials and Methods

2.1. Materials

Eugenol (EU; Product E10439, Canspec, Shanghai, China), medium chain triglyceride (MCT; Neobee-1053, NHG-DMEM, RPMI, Gibco BRL, Life Technologies, Carlsbad, CA, USA), Annexin V/FITC kit (Beyotime, Haimen, Jiangsu, China), Propodium Iodide (PI) were purchased from Life sciences (Beijing, China). Purity Gum Ultra (PGU) was purchased from National starch (Manville, NJ, USA). Bacterial culture Luria Broth agar was purchased from Sigma Aldrich (Saint Louis, MO, USA).

2.2. Preparation of Nano-Emulsion

Eugenol (EU)-loaded nano-emulsions were produced as reported elsewhere [19,20]. Briefly, a lipid phase of a MCT (10%, *v*/*v*) and variable mixed ratios of EU: MCT (1:9, 3:7 and 5:5 (*v*/*v*)) were emulsified with PGU solution (2%, wt/wt) to obtain a coarse emulsion; the mixture was successively passed through a high-pressure homogenizer at a pressure of 150 MPa, and a processing cycles number of 5.

2.3. Particle Size Measurement

Dynamic and phase analysis light scattering (Zetasizer Nano ZS, Malvern Instruments, Malvern, UK) analyses were carried out to measure the emulsion particles size, using 1 mL emulsion samples, after a 100× dilution with deionized water, to avoid multiple light scattering effects. The particle size results for the dynamic light scattering were presented as Z-average mean diameter and polydispersity index (PDI).

2.4. Bacterial Cell Culture and Treatments

E. coli bacteria were taken from GC University Lahore bacterial cell culture lab and were verified via compound microscope. The bacteria were raised in sterile Luria-Bertani (LB) broth and for the flow cytometric enumeration against EU nano-emulsions 10^5 CFU/mL were used. Similarly, *B. breve* and *B. adolescentis* were diluted in a sterile saline

solution (0.9%). De Man, Rogosa and Sharpe agar medium was used to raise both *B. breve* and *B. adolescentis* in anaerobic conditions at 37 °C. Both *E. coli* and beneficial bacteria were treated at 0, 300, 600 and 900 µm EU nano-emulsion to elucidate the bactericidal activity.

2.5. Transmission Electron Microscopy (TEM)

The EU nano-emulsion droplet morphology was examined using digital imaging TEM (JEOL 2100, Hitachi High-Technologies Corp., Tokyo, Japan). EU nano-emulsion drop was deposited on a carbon-coated copper grid via a dropper and dyed using 2% (*w*/*v*) phosphotungstic acid. Before analysis, a drying of the carbon-coated copper grid was performed for 24 h and analyzed via TEM using an accelerating voltage of 100 kV.

2.6. Staining Procedure and Flow Cytometry Analysis

2.6.1. Propidium Iodide (PI) Staining before and after Bulk CO and CO Nano-Emulsions Treatment

PI enters the compromised membrane and interacts with DNA and RNA internally [21]. To study the reversible and permanent permeabilization of *E. coli*, the cells were incubated for 10 min with 30 mM PI to allow the labeling of membrane-compromised cells upon EU nano-emulsion treatment. The excessive PI was removed by washing the cells twice with phosphate-buffered saline buffer.

2.6.2. 5(6)-Carboxyfluorescein Diacetate (CFDA) Staining

CFDA in live cells undergoes nonfluorescent conversion to diacetate via esterases into carboxyfluorescein, a membrane-impermeable fluorescent compound. The presence of carboxyfluorescein in live cells ensures functional cytoplasmic enzymes [21]. The treated EU nano-emulsion, and the control bacterial cells were incubated at 37 °C for 10 min with 50 mM CFDA to promote the CFDA intracellular enzymatic conversion into CF. The excessive CFDA was removed by phosphate-buffered saline washings.

2.6.3. Double Staining

EU nano-emulsion and control bacteria were incubated initially for 10 min in 50 mM CFDA at 37 °C. Later, after CFDA washing via phosphate-buffered saline, bacterial cells were incubated in PI (30 mM) to label/sort out membrane-compromised cells.

2.6.4. Flow Cytometry Analysis

Flow cytometry was performed using FACSCalibur Flow Cytometry (Becton, Dickinson and Company, USA). The flow rate was 400–600 cells/s, with green (FL1) and red fluorescence (FL3) representing CFDA and PI, respectively. The excitation wavelength for CF was 525 nm (FL1 channel), whereas red fluorescence at 620 nm represented PI-labeled cells (FL3 channel). The data obtained was converted into digital signals and interpreted using the software package Expo32 ADC (Beckman-Coulter Inc., Miami, FL, USA). All detectors were calibrated with Flow Check-Fluorospheres (Beckman-Coulter Inc., Miami, FL, USA).

2.7. Fourier Transform Infrared Spectroscopy (FTIR)

A Thermo Fisher Scientific Inc., Nicolet iS10, FTIR spectrometer, equipped with a KBr accessory, was used to acquire the infrared spectra of all samples, in the following conditions: scans number 16, resolution 4 cm^{-1}, wavenumber range of 4000–400 cm^{-1}. The data was obtained using OMNIC software (Version 8.2). For the membrane composition of bacterial cells, the lyophilized bacteria were deposited on a KBr disk. The spectra were acquired.

2.8. Statistical Analysis

The data was analyzed using SPSS Statistics for Windows, version 18.0 (SPSS Inc., Chicago, IL, USA). Analysis of variance (Duncan's multiple range test) was carried out to present the analyzed data of the oil properties in water nano-emulsions. All the values have been presented as Mean ± standard deviation (SD).

3. Results

The considered EU: MCT nano-emulsions were already prepared successfully using high-pressure homogenization by our research group [20]. In the case of 10% MCT oil, the droplet size was >200 nm, whereas it was reduced upon mixing, and reached the smallest value at 5:5% *v*/*v* EU: MCT (i.e., 151.2 ± 1.23 nm) after 5 processing cycles of high-pressure homogenization, as shown in Table 1. This decrease in the droplet is associated with the avoidance of Ostwald ripening due to the mixing of short-chain fatty acids of MCT oil and essential oil (EU). On the other hand, PDI (0.11 ± 0.033) and zeta potential (−28.0 ± 0.19) of 5:5% EU: MCT nano-emulsion were in the best range, confirming the homogeneity and stability of this nano-emulsion formulation. Moreover, to visualize the morphology and droplet size confirmation, TEM is considered a reliable tool for nano-emulsions [22]. TEM analysis also confirmed the spherical morphology of 5:5% EU: MCT nano-emulsion as shown in Figure 1C. However, 1:9 and 3:7 EU: MCT ratios showed oval, non-uniform shapes that endorsed higher polydispersity index values due to Ostwald ripening as shown in Figure 1A,B.

Table 1. Properties of oil in water nano-emulsions prepared with a medium chain triglyceride (MCT) oil phase, purity gum ultra as a surfactant, and 5:5% (*v*/*v*) mixed ratio of each with eugenol.

Emulsion Formulation (*v*/*v*, %)	Particle Size (nm) Mean ± SD	PDI Mean ± SD	Zeta Potential (mV) Mean ± SD	NPS
10% MCT	222.3 ± 5.07 ^{a}	0.11 ± 0.013 ^{a}	−31.1 ± 0.12 ^{a}	5
1:9% EU: MCT	218.2 ± 2.12 ^{a}	0.22 ± 0.10 ^{b}	−27.88 ± 0.08 ^{b}	5
3:7% EU: MCT	180.2 ± 1.22 ^{b}	0.09 ± 0.12 ^{a}	−30.11 ± 0.10 ^{a}	5
5:5% EU: MCT: EU	151.2 ± 1.23 ^{c}	0.11 ± 0.033 ^{a}	−28.0 ± 0.19 ^{b}	5

MCT: medium chain triglyceride oil, EU: eugenol, PDI: polydispersity index, NPS: number of processing cycles, SD: standard deviation. Values with the different superscript letters (within a column) are significantly different.

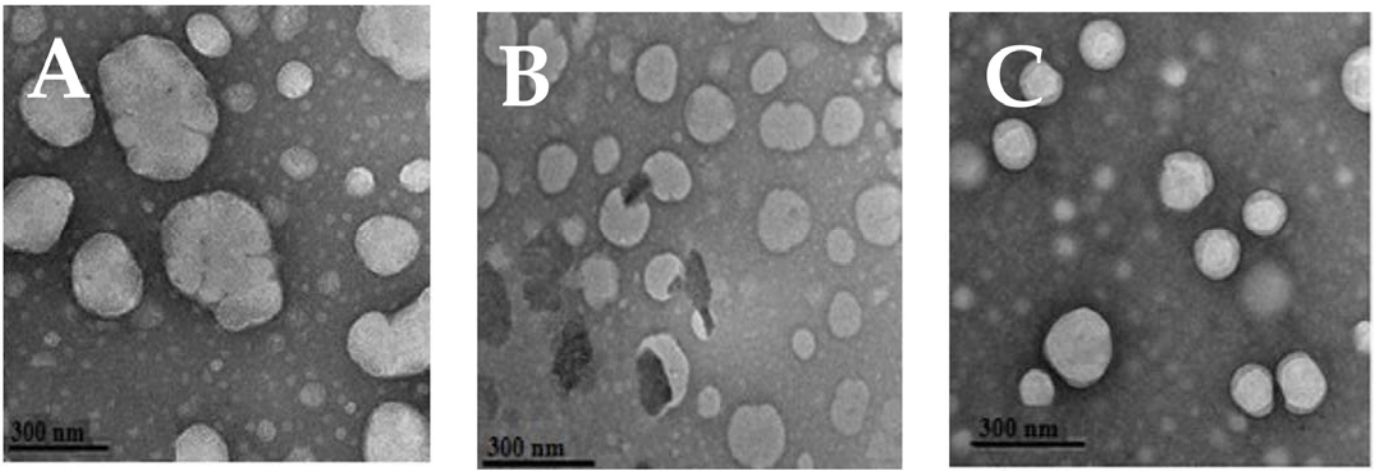

Figure 1. Transmission electron microscopy (TEM) of eugenol (EU) nano-emulsion prepared with 1:9 (**A**), 3:7 (**B**) and 5:5 (**C**) EU: MCT oil ratio.

Furthermore, these EU nano-emulsions have shown superior antibacterial activity against pathogenic Gram-positive (*S. aureus* and *L. monocytogenes*) and negative bacteria (*E. coli*), as presented in our previous work [20]. The current research focus was to evaluate the impacts of these EU nano-emulsions on beneficial gut bacteria such as *B. breve* and *B. adolescentis*. Therefore, we selected 0, 300, 600 and 900 µm of EU nano-emulsions as the effective concentration against liver and colon cancer cell lines was around 300 µm [18]. We decided to evaluate the effect of these EU nano-emulsions against both pathogenic resistant (*E. coli*) and beneficial bacteria (*B. breve* and *B. adolescentis*). Time kill dynamic plots of *B. breve* and *B. adolescentis* at 0, 300, 600 and 900 µm EU nano-emulsions are presented in Figure 2. In the case of control, the *B. breve* and *B. adolescentis* showed normal growth

patterns. The bacteria number rose from 10^3 CFU/mL to 10^7 after 36 h (Figure 2A,B). Similarly, both *B. breve* and *B. adolescentis* showed the same trend of no growth inhibition when treated with 300, 600 and 900 µm EU nano-emulsion (Figure 2A,B).

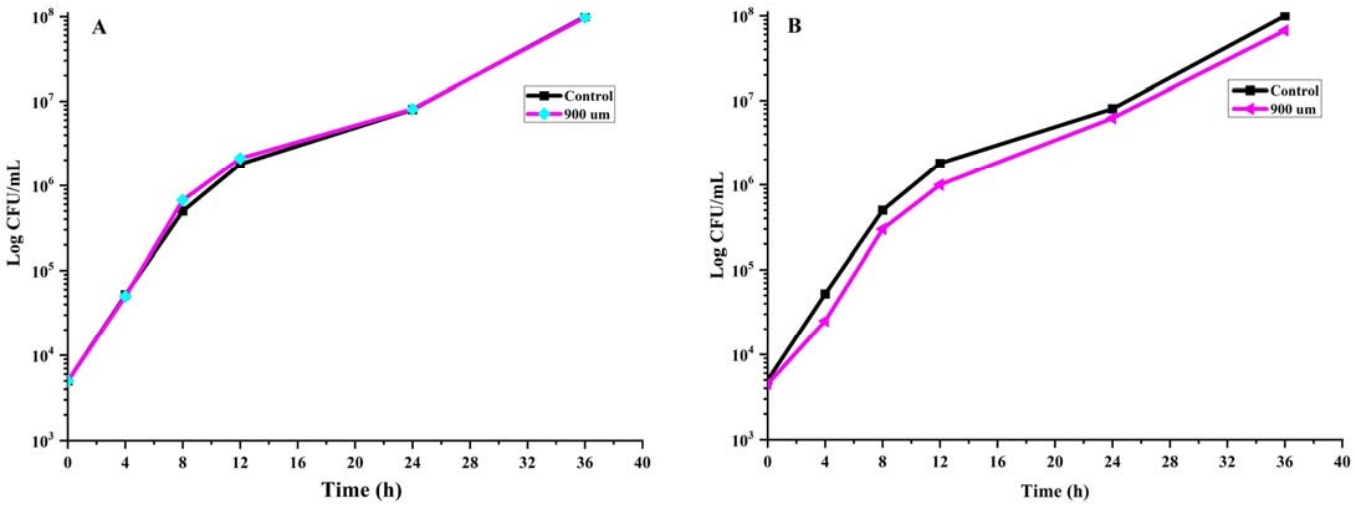

Figure 2. Time kill dynamics of *B. breve* and *B. adolescentis* upon treatment with 0, 300, 600 and 900 µm EU nano-emulsion. Only 0 and 900 µm concentration effects on growth have been shown to avoid overlapping, as there was no reduction in the growth of *B. breve* (**A**) and *B. adolescentis* (**B**) at any treatment.

To further clarify the plate count method, flow cytometry was performed to distinguish the live (R2), membrane damaged (R3) and sublethal bacterial cells (R4) of both pathogenic resistant *E. coli* and beneficial *B. breve* and *B. adolescentis*. Similarly, flow cytometry CFDA vs PI dot plot was utilized to distinguish subpopulations of *Lactobacillus* and *Bifidobacterium* sp. in commercial powders [23–25]. As shown in Figure 3, the *B. breve* showed no damaged (R3) or sublethal (R4) population in the case of the control (Figure 3A). Upon the treatment with 300 µm EU nano-emulsion, the live cells (R2) percentage was 93.84%, R4 0.14%, R3 0.01%. The shifting of live cells R2 to sublethal R4 suggests revivable bacterial cells due to a higher dose. However, at 300, 600 and 900 µm EU nano-emulsion treatment, the R3 (membrane-damaged) bacterial cells percentage was 0%, suggesting no bacterial inhibition at these doses. Similarly, a gut microbiota flora improvement was reported when rats were fed with sweet orange microcapsules [26]. The maximum percentage of sublethal bacterial cells was 0.51% when treated with 900 µm EU nano-emulsion (Figure 3D). The membrane-damaged bacterial quadrant R3 percentage was 0% (Figure 4A–C). In the case of *B. adolesentis*, the maximum percentage of sublethal bacterial cells after 36 h of treatment was 0.15% (Figure 4C). These results suggest the safety of EU nano-emulsions up to the mentioned doses against the gut-beneficial microbiota.

Similarly, such as beneficial gut microbiota (*B. breve* and *B. adolescentis*) enumeration via flow cytometry, the resistant pathogenic *E. coli* bacterial cells upon treatments with 0, 300, 600 and 900 µm EU nano-emulsions were also categorized into subpopulations: R2 (live), R4 (sub-lethal), R3 (membrane-damaged) and R1 (debris) (Figure 5). Majeed et al. utilized the FITC versus PI flow cytometry dot plot to categorize *E. coli*, *L. monocytogenes*, and *S. aureus* subpopulations upon treatment with clove oil nano-emulsions [18]. The *E. coli* bacterial cells in the absence of EU nano-emulsion showed a maximum percentage of live subpopulation in the R2 quadrant (99.20%). Upon treatment with 300 µm EU nano-emulsion, the live subpopulation (R2) shifted to R3 (membrane-damaged), which accounts for 99.18% after 36 h of treatment. On the other hand, the sublethal subpopulation was 0.82%, as shown in Figure 5B. Further, resistant *E. coli* when treated with 600 and 900 µm EU nano-emulsion showed more percentage of the R3 quadrant (99.92%), suggesting superior efficacy against resistant *E. coli*.

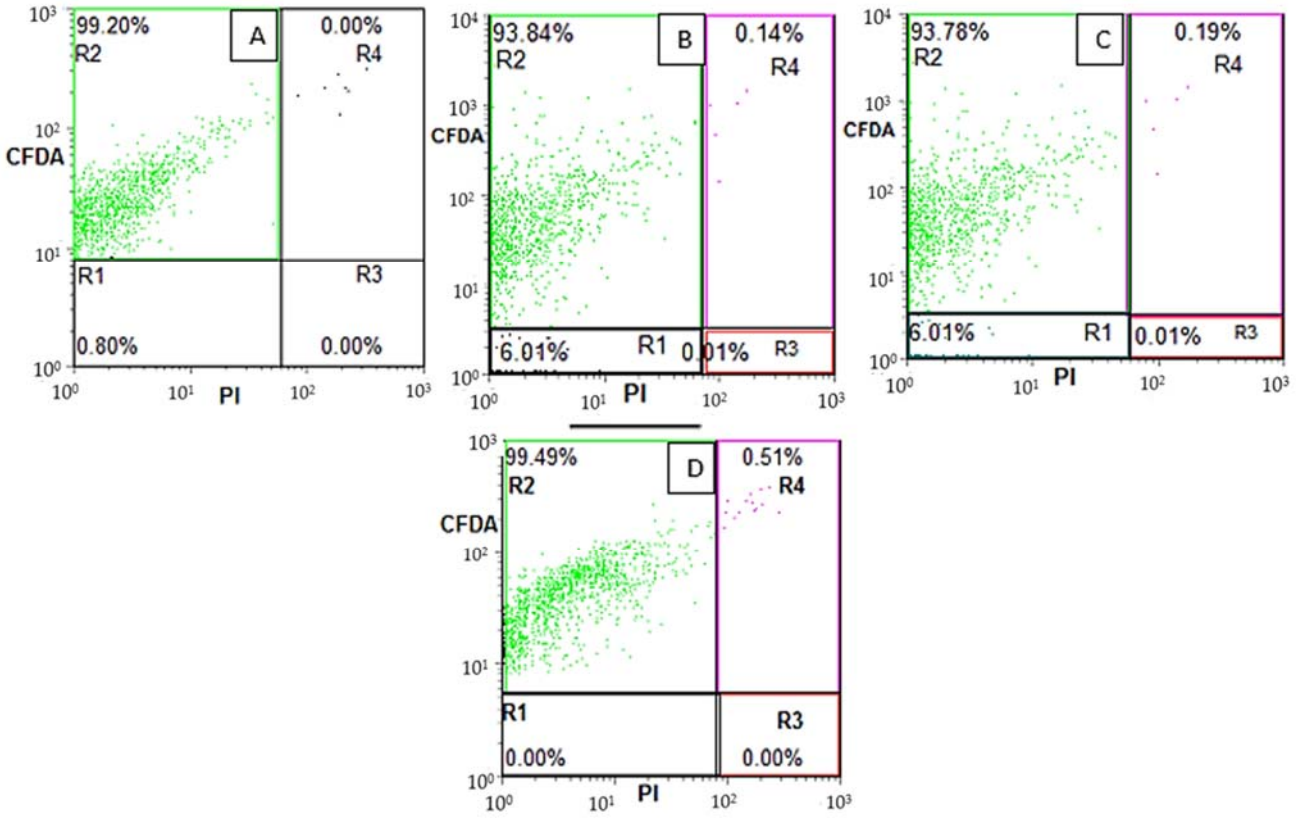

Figure 3. Flow cytometric dot plots of *B. breve* upon treatment with 0 (**A**), 300 (**B**), 600 (**C**) and 900 (**D**) μm EU nano-emulsion after 36 h of treatment. R1 (cell debris), R2 (viable cells), R3 (membrane-damaged cells) and R4 (sub-lethal cells).

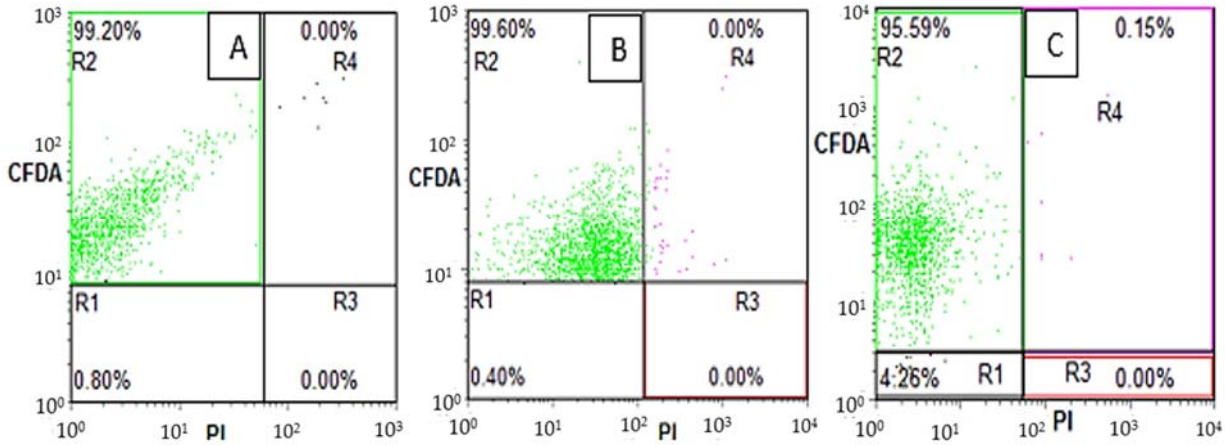

Figure 4. Flow cytometric dot plots of *B. adolescentis* upon treatment with 300 (**A**), 600 (**B**) and 900 (**C**) μm EU nano-emulsion after 36 h of treatment. R1 (cell debris), R2 (viable cells), R3 (membrane-damaged cells) and R4 (sub-lethal cells).

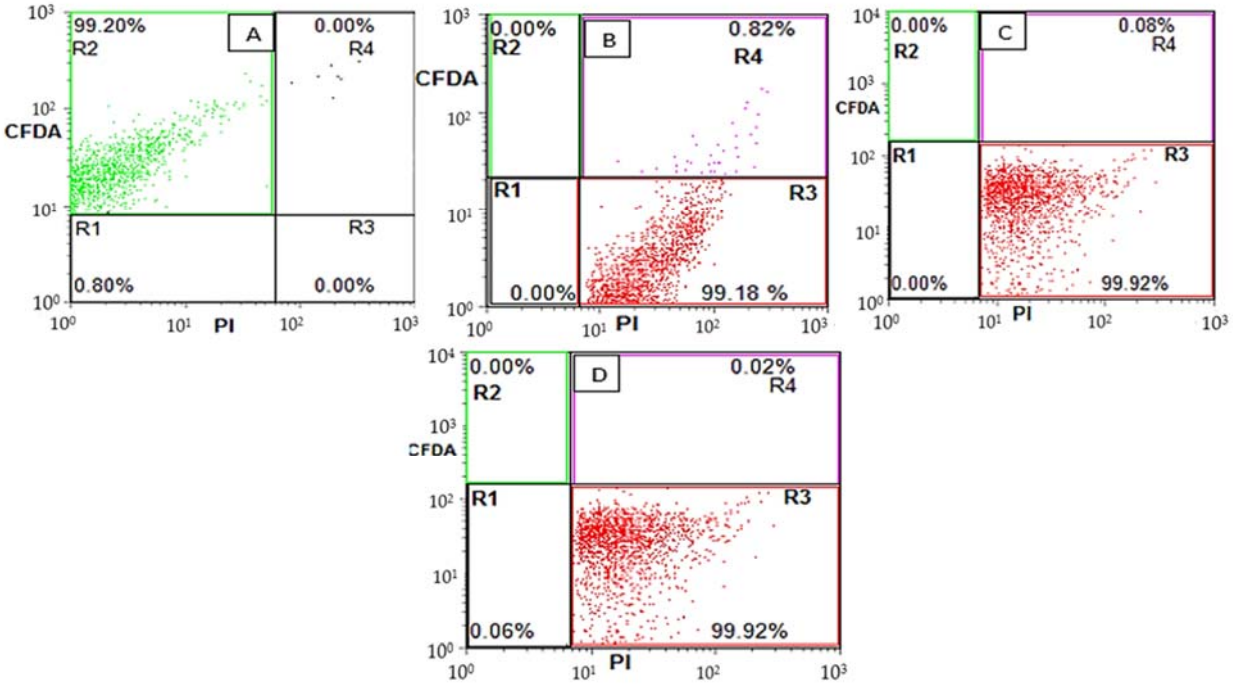

Figure 5. Flow cytometric dot plot distribution of *E. coli* bacteria upon treatment with 0 (**A**), 300 (**B**), 600 (**C**) and 900 (**D**) µm EU nano-emulsion after 36 h of treatment. R1 (cell debris), R2 (viable cells), R3 (membrane-damaged cells) and R4 (sublethal cells).

Due to the presence of a sublethal subpopulation (R4) of *B. breve* and *B. adolescentis* upon treatment with EU nano-emulsion at 900 µm, the FTIR was performed to evaluate the membrane composition change to judge the revivable bacteria. Figure 6 depicts the FTIR spectra of the untreated *B. breve* and *B. adolescentis* (in black, control) having intact membrane composition proteins (3250 cm^{-1}), lipids (2000–3000 cm^{-1}), DNA (1200–1400 cm^{-1}) and carbohydrates (1000 cm^{-1}). Both *B. breve* and *B. adolescentis* upon treatment with EU nano-emulsion at 900 µm showed similar membrane composition as appeared in non-treated (control) (Figure 6).

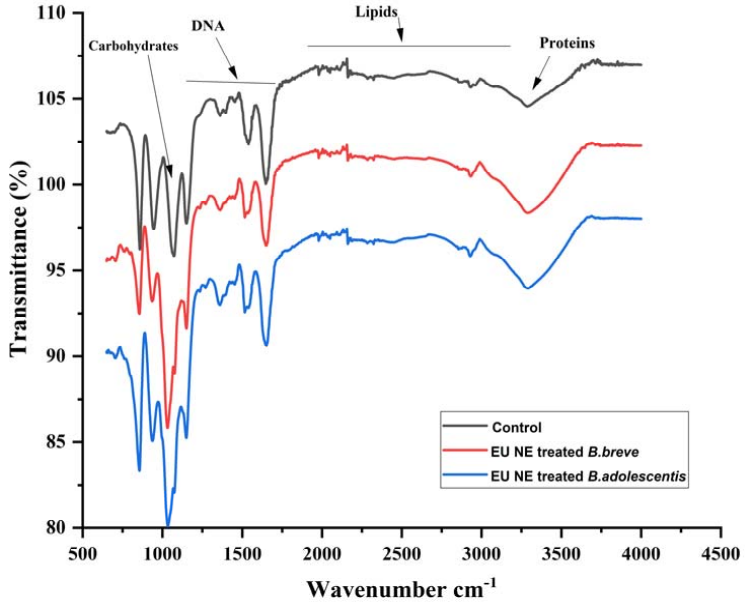

Figure 6. FTIR spectra of *B. breve* and *B. adolescentis* untreated (control) and treated with EU nano-emulsion (900 µm) to elucidate the change in the membrane chemical composition.

On the other hand, the lowest sublethal population (R4) percentage of 0.02% of resistant *E. coli* suggests no revivable bacterial cells. Therefore, FTIR analysis revealed a complete compositional change of resistant *E. coli* upon treatment with 900 µm EU nano-emulsion (Figure 7). The untreated (control) *E. coli* is characterised by lipids (2900–2750 cm^{-1}), proteins (1600 cm^{-1}) and DNA (1500–1250 cm^{-1}). The EU nano-emulsion-treated *E. coli* at 900 µm showed a clear sharp shift in lipids, proteins, and DNA, as shown in Figure 7 (Red line), while carbohydrates showed a clear shift in peak intensity from 1000 to 1020 cm^{-1}.

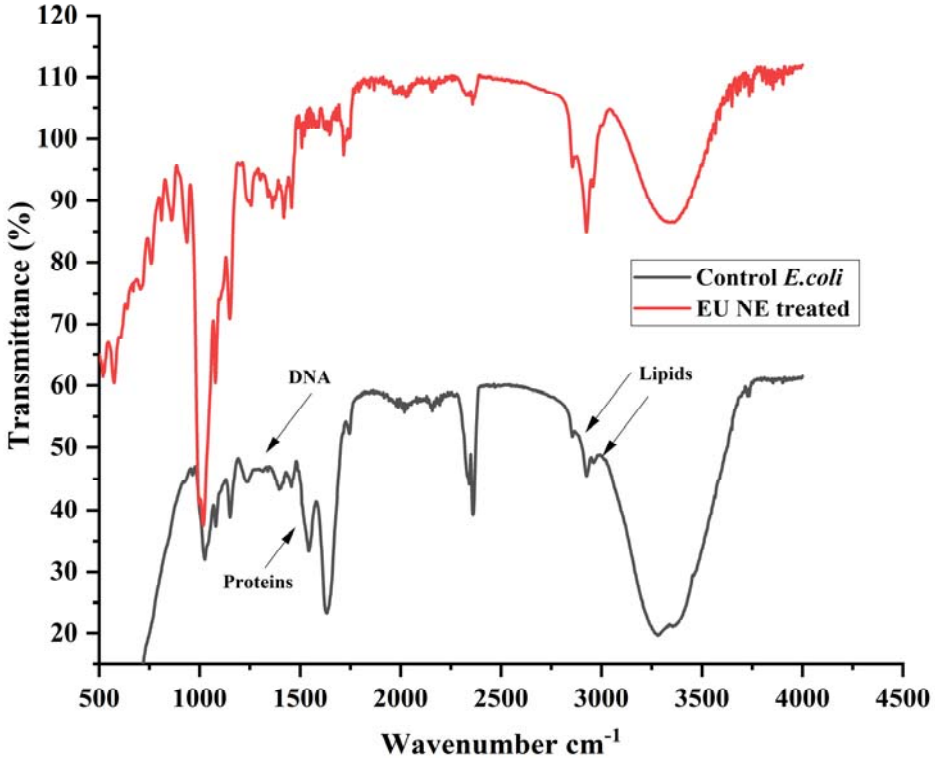

Figure 7. FTIR spectra of *E. coli* untreated (control) and treated with EU nano-emulsion (900 µm) to elucidate the change in membrane chemical composition.

4. Discussions

Among the lipid encapsulation systems, the most commercially viable one is the nano-emulsion, being kinetically stable and requiring less usage of emulsifiers [7]. Nano-emulsions of essential oils have been formulated to enhance their solubility and bioavailability. Liang et al. prepared peppermint oil-loaded nano-emulsions via high-pressure homogenization and reported droplet size < 200 nm. Interestingly, the small-sized nano-emulsion was more effective against Gram-positive (*L. monocytogenes*) bacteria [13]. The droplet size of the nano-emulsion could be controlled with the addition of medium-chain or long-chain triglycerides in the oil phase, preventing the Ostwald ripening [20,27]. In our current formulation, an EU-loaded nano-emulsion of 150 nm droplet size was prepared with the addition of MCT oil as an Ostwald ripening inhibitor.

Nano-emulsion droplet size reduced with increasing homogenization cycles. The same phenomenon has been reported in various research [6,7,12]. A similar phenomenon has been observed in the current study: the smallest droplet size of EU nano-emulsion was prepared at five homogenization processing cycles. PDI with an increasing number of homogenization processing cycles also reduced, as shown in Table 1. The possible reason behind this phenomenon is the homogeneity of nano-emulsion droplets [12]. The minimum acceptable PDI value is <0.3 nm. In our case, with five processing cycles, the PDI values are below 0.1 nm. In addition to particle size and PDI, zeta potential of nano-emulsion also possesses prime importance in successful preparation. The negative charge zeta potential

value showed a more stable formulation. We prepared <200 nm droplet size nano-emulsion having −28 mV zeta potential value. Similar, stable nano-emulsion formulations having negative charge zeta potential values were more stable.

The essential oil-loaded nano-emulsion was successfully used as an antibacterial agent against Gram-positive and Gram-negative bacteria [7,20]. Ambrosio et al. evaluated essential oils (*Eucalyptus globulus*, orange oil, citrus terpens) activity against resistant pathogenic bacteria *S. entritidis*, *S. aureus*, *E. coli* and beneficial bacteria *L. rhamnosus*, using the plate count method [28]. They confirmed more inhibition of pathogenic strains and less/no inhibition of *L. rhamnosus*. Similarly, other researchers also reported less inhibitory effects of essential oils/constituents against beneficial bacteria [4].

The plate count method illustrates a decrease in the colony-forming unit of pathogenic or beneficial bacteria, which is not enough to judge the efficacy of antimicrobial or growth stimulators [29,30]. Various researchers used the flow cytometry to distinguish live, dead and sublethal bacterial populations upon treatment with antimicrobials [31]. Similarly, flow cytometric subpopulations of live, membrane damaged, and sublethal pathogenic bacteria (*S. aureus* and *E. coli*) after treatment with eugenol, chitooligosaccharide and celery essential oil were successfully characterized to judge the efficacy of the antimicrobial compounds in vivo [32]. With the flow cytometry advent, it is easier to distinguish culturable and non-culturable beneficial bacteria for various food or nutraceutical formulations. Additionally, this technique would be an advantage for beneficial bacteria-enriched food during storage. In our findings, *B. breve* and *B. adolescentis* showed a very less percentage of the sublethal population (revivable) upon treatment with 900 µm EU nano-emulsion, suggesting less inhibitory potential. Sublethal bacteria could revive back to normal with no compromised membrane. To justify the membrane composition change, various researchers used FTIR to analyze the changes in the protein, lipids, DNA and carbohydrates of bacteria upon treatment with antimicrobials. Parvarei et al. used FTIR to characterize the suitable spectral regions for *Bifidobacterium* sp. [33]. FTIR was also utilized to characterize the membrane components for their proper application in foods [34]. Similarly, a membrane compositional change was reported in *A. baumannii* upon treatment with chlorhexidine as elucidated via FTIR [35,36].

5. Conclusions

The current study has provided flow cytometry combined with cell sorting as an efficient tool to not only distinguish live and dead cells, but also to separate bacteria as per its physiological state. The flow cytometry and FTIR could be suitable approaches to not only judge the suitability of antibacterial agents against resistant bacteria, but also help determine the sensitivity of gut-beneficial bacteria. Further, this approach will help to evaluate probiotics' safety in food and nutraceuticals during storage. Thus, the present work provides an analytical tool to characterize resistant and beneficial bacteria upon treatment with antimicrobials, and will help to choose antimicrobials for a safe food chain supply.

Author Contributions: Conceptualization, U.M. and A.S.; methodology, M.S.; software, U.M.; validation, K.u.R.K., U.M. and K.J.I.; formal analysis, U.M. and K.A.; investigation, I.B. and U.M.; resources, S.H.M., I.C., M.M.M. and S.A.K.; data curation, U.M., I.C., T.E. and S.A.K.; writing—original draft preparation, U.M.; writing—review and editing, R.S., H.M., I.C., T.E. and S.A.K.; visualization, U.M., S.H.M., T.E. and S.A.K.; supervision, U.M.; project administration, U.M., A.S. and S.A.K.; funding acquisition, K.u.R.K., T.E. and S.A.K. All authors have read and agreed to the published version of the manuscript.

Funding: The publication of this article was supported by the Open Access Fund of Leibniz Universität Hannover. The authors thanks Pakistan Science Foundation funded project, grant No: PSF/CRP/TH/4/CFP/430 for their support.

Institutional Review Board Statement: Not applicable.

Informed Consent Statement: Not applicable.

Data Availability Statement: Data will be provided on demand.

Conflicts of Interest: The authors declare no conflict of interest.

References

1. Maurya, V.K.; Gothandam, K.M.; Ranjan, V.; Shakya, A.; Pareek, S. Effect of drying methods (microwave vacuum, freeze, hot air and sun drying) on physical, chemical and nutritional attributes of five pepper (*Capsicum annuum* var. *annuum*) cultivars. *J. Sci. Food Agric.* **2018**, *98*, 3492–3500. [CrossRef] [PubMed]
2. Unalan, I.; Boccaccini, A.R. Essential oils in biomedical applications: Recent progress and future opportunities. *Curr. Opin. Biomed. Eng.* **2021**, *17*, 100261. [CrossRef]
3. Mansouri, S.; Pajohi-Alamoti, M.; Aghajani, N.; Bazargani-Gilani, B.; Nourian, A. Stability and antibacterial activity of *Thymus daenensis L.* essential oil nanoemulsion in mayonnaise. *J. Sci. Food Agric.* **2021**, *101*, 3880–3888. [CrossRef] [PubMed]
4. Ouwehand, A.; Tiihonen, K.; Kettunen, H.; Peuranen, S.; Schulze, H.; Rautonen, N. In vitro effects of essential oils on potential pathogens and beneficial members of the normal microbiota. *Vet. Med.* **2010**, *55*, 71–78. [CrossRef]
5. Thapa, D.; Losa, R.; Zweifel, B.; Wallace, R.J. Sensitivity of pathogenic and commensal bacteria from the human colon to essential oils. *Microbiology* **2012**, *158*, 2870–2877. [CrossRef]
6. Yang, Z.; He, Q.; Ismail, B.B.; Hu, Y.; Guo, M. Ultrasonication induced nano-emulsification of thyme essential oil: Optimization and antibacterial mechanism against *Escherichia coli*. *Food Control.* **2022**, *133*, 108609. [CrossRef]
7. da Silva, B.D.; Rosario, D.K.A.D.; Conte-Junior, C.A. Can droplet size influence antibacterial activity in ultrasound-prepared essential oil nanoemulsions? *Crit. Rev. Food Sci. Nutr.* **2022**, 1–11. [CrossRef]
8. Al-Otaibi, W.A.; AlMotwaa, S.M. Preparation, characterization, optimization, and antibacterial evaluation of nano-emulsion incorporating essential oil extracted from *Teucrium polium* L. *J. Dispers. Sci. Technol.* **2021**, 1–11. [CrossRef]
9. Sharma, A.D.; Kaur, I.; Singh, N. Synthesis, Characterization, and *in vitro* drug release and *in vitro* antibacterial activity of o/w nanoemulsions loaded with natural eucalyptus globulus essential oil. *J. Nanosci. Nanotechnol.* **2021**, *17*, 191–207.
10. Roozitalab, G.; Yousefpoor, Y.; Abdollahi, A.; Safari, M.; Rasti, F.; Osanloo, M. Antioxidative, anticancer, and antibacterial activities of a nanoemulsion-based gel containing *Myrtus communis* L. essential oil. *Chem. Papers* **2022**, *76*, 4261–4271. [CrossRef]
11. Zhu, Y.; Li, C.; Cui, H.; Lin, L. Encapsulation strategies to enhance the antibacterial properties of essential oils in food system. *Food Control* **2021**, *123*, 107856. [CrossRef]
12. Mao, L.; Xu, D.; Yang, J.; Yuan, F.; Gao, Y.; Zhao, J. Effect of small and large molecules emulsifiers on the characteristics of b-carotene nanoemulsions prepared by high pressure homogenization. *Food Technol. Biotechnol.* **2009**, *47*, 336–342.
13. Liang, R.; Xu, S.; Shoemaker, C.F.; Li, Y.; Zhong, F.; Huang, Q. Physical and antimicrobial properties of peppermint oil nanoemulsions. *J. Agric. Food Chem.* **2012**, *60*, 7548–7555. [CrossRef] [PubMed]
14. Donsì, F.; Annunziata, M.; Vincensi, M.; Ferrari, G. Design of nanoemulsion-based delivery systems of natural antimicrobials: Effect of the emulsifier. *J. Biotechnol.* **2012**, *159*, 342–350. [CrossRef] [PubMed]
15. Terjung, N.; Löffler, M.; Gibis, M.; Hinrichs, J.; Weiss, J. Influence of droplet size on the efficacy of oil-in-water emulsions loaded with phenolic antimicrobials. *Food Funct.* **2012**, *3*, 290–301. [CrossRef]
16. Lin, Y.-E.; Lin, M.-H.; Yeh, T.-Y.; Lai, Y.-S.; Lu, K.-H.; Huang, H.-S.; Peng, F.-C.; Liu, S.-H.; Sheen, L.-Y. Genotoxicity and 28-day repeated dose oral toxicity study of garlic essential oil in mice. *J. Tradit. Complement. Med.* **2022**, *12*, 536–544. [CrossRef]
17. Wang, Q.; Gong, J.; Huang, X.; Yu, H.; Xue, F. *In vitro* evaluation of the activity of microencapsulated carvacrol against *Escherichia coli* with K88 pili. *J. Appl. Microbiol.* **2009**, *107*, 1781–1788. [CrossRef]
18. Majeed, H.; Antoniou, J.; Fang, Z. Apoptotic effects of eugenol-loaded nanoemulsions in human colon and liver cancer cell lines. *Asian Pac. J. Cancer Prev.* **2014**, *15*, 9159–9164. [CrossRef]
19. Majeed, H.; Antoniou, J.; Shoemaker, C.F.; Fang, Z. Action mechanism of small and large molecule surfactant-based clove oil nanoemulsions against food-borne pathogens and real-time detection of their subpopulations. *Arch. Microbiol.* **2015**, *197*, 35–45. [CrossRef]
20. Majeed, H.; Liu, F.; Hategekimana, J.; Sharif, H.R.; Qi, J.; Ali, B.; Bian, Y.-Y.; Ma, J.; Yokoyama, W.; Zhong, F. Bactericidal action mechanism of negatively charged food grade clove oil nanoemulsions. *Food Chem.* **2016**, *197*, 75–83. [CrossRef]
21. Zhao, W.; Yang, R.; Zhang, H.Q.; Zhang, W.; Hua, X.; Tang, Y. Quantitative and real time detection of pulsed electric field induced damage on *Escherichia coli* cells and sublethally injured microbial cells using flow cytometry in combination with fluorescent techniques. *Food Control.* **2011**, *22*, 566–573. [CrossRef]
22. Ju, S.-N.; Shi, H.-H.; Yang, J.-Y.; Zhao, Y.-C.; Xue, C.-H.; Wang, Y.-M.; Huang, Q.-R.; Zhang, T.-T. Characterization, stability, digestion and absorption of a nobiletin nanoemulsion using DHA-enriched phosphatidylcholine as an emulsifier in vivo and in vitro. *Food Chem.* **2022**, *397*, 133787. [CrossRef]
23. Sielatycka, K.; Juzwa, W.; Śliwa-Dominiak, J.; Kaczmarczyk, M.; Łoniewski, I.; Marlicz, W. Multiparameter flow cytometric enumeration of probiotic-containing commercial powders. *Innov. Food Sci. Emerg. Technol.* **2021**, *68*, 102598. [CrossRef]
24. Michelutti, L.; Bulfoni, M.; Nencioni, E. A novel pharmaceutical approach for the analytical validation of probiotic bacterial count by flow cytometry. *J. Microbiol. Method* **2020**, *170*, 105834. [CrossRef] [PubMed]

25. da Cruz Rodrigues, V.C.; da Silva, L.G.S.; Simabuco, F.M.; Venema, K.; Antunes, A.E.C. Survival, metabolic status and cellular morphology of probiotics in dairy products and dietary supplement after simulated digestion. *J. Funct. Foods* **2019**, *55*, 126–134. [CrossRef]
26. Porat, R.; Lichter, A.; Terry, L.A.; Harker, R.; Buzby, J. Postharvest losses of fruit and vegetables during retail and in consumers' homes: Quantifications, causes, and means of prevention. *Postharvest Biol. Technol.* **2018**, *139*, 135–149. [CrossRef]
27. Hou, K.; Xu, Y.; Cen, K.; Gao, C.; Feng, X.; Tang, X. Nanoemulsion of cinnamon essential oil Co-emulsified with hydroxypropyl-β-cyclodextrin and Tween-80: Antibacterial activity, stability and slow release performance. *Food Biosci.* **2021**, *43*, 101232. [CrossRef]
28. Ambrosio, C.M.S.; de Alencar, S.M.; de Sousa, R.L.M.; Moreno, A.M.; Da Gloria, E.M. Antimicrobial activity of several essential oils on pathogenic and beneficial bacteria. *Ind. Crops Prodct.* **2017**, *97*, 128–136. [CrossRef]
29. Fu, X.; Gao, Y.; Yan, W.; Zhang, Z.; Sarker, S.; Yin, Y.; Liu, Q.; Feng, J.; Chen, J. Preparation of eugenol nanoemulsions for antibacterial activities. *RSC Adv.* **2022**, *12*, 3180–3190. [CrossRef]
30. Krithika, B.; Preetha, R. Formulation of protein based inulin incorporated synbiotic nanoemulsion for enhanced stability of probiotic. *Mater. Res. Express* **2019**, *6*, 114003. [CrossRef]
31. Meng, L.; Ma, J.; Liu, C.; Mao, X.; Li, J. The microbial stress responses of *Escherichia coli* and *Staphylococcus aureus* induced by chitooligosaccharide. *Carbohydr. Polym.* **2022**, *287*, 119325. [CrossRef] [PubMed]
32. Nirmala, M.J.; Durai, L.; Gopakumar, V.; Nagarajan, R. Preparation of celery essential oil-based nanoemulsion by ultrasonication and evaluation of its potential anticancer and antibacterial activity. *Int. J. Nanomed.* **2020**, *15*, 7651. [CrossRef] [PubMed]
33. Parvarei, M.M.; Khorshidian, N.; Fazeli, M.R.; Mortazavian, A.M.; Nezhad, S.S.; Mortazavi, S.A. Comparative effect of probiotic and paraprobiotic addition on physicochemical, chemometric and microstructural properties of yogurt. *LWT-Food Sci. Technol.* **2021**, *144*, 111177. [CrossRef]
34. Amiri, S.; Rezazadeh-Bari, M.; Alizadeh-Khaledabad, M.; Rezaei-Mokarram, R.; Sowti-Khiabani, M. Fermentation optimization for co-production of postbiotics by *Bifidobacterium lactis* BB12 in cheese whey. *Waste Biomass Valorization* **2021**, *12*, 5869–5884. [CrossRef]
35. Biswas, D.; Tiwari, M.; Tiwari, V. Molecular mechanism of antimicrobial activity of chlorhexidine against carbapenem-resistant *Acinetobacter baumannii*. *PLoS ONE* **2019**, *14*, e0224107. [CrossRef]
36. Ansari, M.A.; Khan, H.M.; Khan, A.A.; Ahmad, M.K.; Mahdi, A.A.; Pal, R.; Cameotra, S.S. Interaction of silver nanoparticles with *Escherichia coli* and their cell envelope biomolecules. *J. Basic Microbiol.* **2014**, *54*, 905–915. [CrossRef] [PubMed]